

HIGHLY SCALABLE NUMERICAL METHODS FOR SIMULATION OF SPACE CHARGE DOMINATED BEAMS *

J. Xu[#], B. Mustapha, P. N. Ostroumov, and J. A. Nolen, Argonne National Laboratory, Argonne, IL 60439, USA

ABSTRACT

Beam dynamic simulations with kinetic model have been conducted. We have successfully parallelized a PIC solver, TRACK, and developed new Vlasov solvers. For the PIC solver, particles are distributed evenly on different processors and space charge effect has been counted by solving Poisson's equation on a finite mesh. Several Poisson solvers have been developed using Fourier method in Cartesian coordinate system, Fourier Spectral Element in Cylindrical coordinate system, Wavelet method, Spectral Element Method (SEM) on structured and unstructured grids. Domain decomposition (DD) has been used to parallelize these solvers. Different Poisson solvers have been developed for simulating space charge dominated beams. These solvers have been incorporated into PTRACK and Vlasov solvers. PTRACK has now widely been used for large scale beam dynamics simulations in linear accelerators. For the Vlasov solver, Semi-Lagrangian method and time splitting scheme have been employed to solve Vlasov equation directly in 1P1V and 2P2V phase spaces. Similarly, DD has been used for parallelization of Vlasov solvers.

INTRODUCTION

Plasma and charged particle simulations have great importance in science. There are three different approaches to simulate plasmas: the microscopic model, the kinetic model and the fluid model. In the microscopic model, each charged particle is described by 6 variables (x, y, z, v_x, v_y, v_z). Therefore, for N particles, there are $6N$ variables in total. This requires solving the Vlasov equation in $6N$ dimensions, which exceeds the capability of current supercomputers for large N . On the other end is the fluid model which is the simplest because it treats the plasma as a conducting fluid with electromagnetic forces exerted on it. This leads to solving the Magneto-hydrodynamics (MHD) equations in 3D (x, y and z). MHD solves for the average quantities, such as density and charge, which makes it difficult to describe the fine structure in the plasma. Between these two models is the kinetic model, which solves for the charge density function by solving the Boltzmann or Vlasov equations in 6 dimensions (x, y, z, v_x, v_y, v_z). The Vlasov equation describes the evolution of a system of particles under the effects of self-consistent electromagnetic fields. This paper deals with the kinetic model.

There are two different ways to solve the kinetic model. The most popular one is to represent the beam bunch by macro particles and push the macro particles along the characteristics of the Vlasov equation. This is the so called Particle-In-Cell (PIC) method, which utilizes the motion of the particles along the characteristics of the Vlasov equation using a Lagrange-Euler approach [1, 2]. The PIC method has the advantages of speed and easy implementation, but similar to MHD, it is hard to calculate fine structures in the plasma. Furthermore, there is noise associated with the finite number of particles in the simulation. This noise decreases very slowly, as $1/\sqrt{N}$, when the number of particles N is increased. The other way to solve the kinetic model is to solve the Vlasov equation directly. This can overcome the shortcomings of the PIC method. We have applied SEM which can achieve high order accuracy and developed scalable Poisson and Vlasov solvers. This paper reports our work using both models. In order to describe space charge effects, several Poisson solvers have been developed.

BEAM DYNAMIC SIMULATION WITH PIC SOLVER

In the last several years, we have parallelized a PIC solver, TRACK, which has been developed in physics division at ANL. Parallel algorithm and detailed benchmark results can be in [2, 3, 4]. Recently PTRACK has been used for an one-to-one RFQ simulation of FNAL proton driver. Totally 865M charged particles have been simulated from 50 keV to 2.5 MeV in 325 MHz radio frequency quadrupole of a proton driver at FNAL. Figure 1 is the comparison in ($\phi, \Delta W/W$) plane. This result provides much more accurate information and useful to the design optimizations. Now PTRACK has been used as workhorse for large scale optimizations.

PARALLEL POISSON SOLVERS

Fourier Method

$$\phi(x, y, z, t) = \sum_{m=-M/2}^{M/2-1} \sum_{p=-P/2}^{P/2-1} \sum_{n=-N/2}^{N/2-1} \phi(m, p, n, t) e^{-iamx} e^{-i\beta py} e^{-in z}$$

This is the most standard method for solving the Poisson's equation in Cartesian coordinate system. The potential has been expanded in Fourier series in all three directions. Periodic and Dirichlet zero boundary conditions have been applied in all three directions. Three different domain decomposition methods have been implemented as shown in Fig.2. Using model C, it is easy to use tens of thousands of processors with relatively small grid for space charge calculation. Since

* This work was supported by the U.S. Department of Energy, Office of Nuclear Physics, under Contract No. DE-AC02-06CH11357.

[#]jin_xu@anl.gov

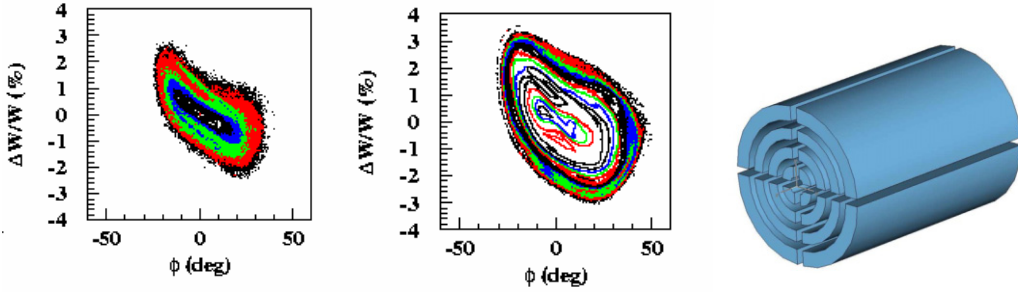


Fig. 1: Phase contour comparison in $(\phi, \Delta W/W)$ plane and parallel model in cylinder coordinate system

relatively small grid can be used for space charge calculation, good scaling has been obtained and can be found in [3, 4].

Fourier Spectral Element Method

This solver is developed for cylinder coordinate system. The potential is expanded in Fourier series in the axial and circumferential directions, while it uses spectral element expansion in the radial direction.

$$\phi(x, y, z, t) = \sum_{m=-M/2}^{M/2-1} \sum_{n=-N/2}^{N/2-1} \sum_0^P \phi(m, p, n, t) e^{-iamx} e^{-i\beta nz} P_p(y)$$

$$P_p(y) = \begin{cases} \left(\frac{1-y}{2}\right) & p = 0 \\ \left(\frac{1-y}{2}\right)\left(\frac{1+y}{2}\right)P_{p-1}^{1,1}(y) & 0 < p < P \\ \left(\frac{1+y}{2}\right) & p = P \end{cases}$$

Domain decomposition in the radial and circumferential directions has been implemented as shown in the right of Fig. 1. Periodic B.C. has been applied in the axial and circumferential directions and zero Dirichlet B.C. have been applied in the cylinder wall. Detailed method and benchmark results can be found in [2].

Wavelet Method

Recently, multi-resolution analysis (MRA) emerges

$$V_j = \{\phi_{j,k}, k \in Z\} \quad \phi_{j,k}(x) = 2^{j/2} \phi(2^j x - k)$$

$$\dots \subset V_{-2} \subset V_{-1} \subset V_0 \subset V_1 \subset V_2 \subset \dots \subset L^2(R)$$

Since $V_j \supset V_{j+1}$, we can define $W_j \perp V_j$ and $W_j \supset V_{j+1}$, such that $V_j \oplus W_j = V_{j+1}$, where

$$W_j = \{\psi_{j,k}, k \in Z\} \quad \psi_{j,k}(x) = 2^{j/2} \psi(2^j x - k)$$

Then

$$V_2 = W_1 \oplus V_1 = W_1 \oplus W_0 \oplus V_0$$

$$= W_1 \oplus W_0 \oplus W_{-1} \oplus V_{-1}$$

There is an efficient preconditioning matrix for the linear system generated by the wavelet expansion. We use following analytical solution to test this wavelet Poisson solver.

$$\phi(x, y, z) = (x + \pi)(x - 3\pi)$$

$$(y + \pi)(y - 3\pi)(z + \pi)(z - 3\pi)$$

$$\Delta \phi(x, y, z) = -\rho(x, y, z)$$

$$\rho(x, y, z) = 2(x + \pi)(x - 3\pi)(y + \pi)(y - 3\pi)$$

$$+ 2(x + \pi)(x - 3\pi)(z + \pi)(z - 3\pi)$$

$$+ 2(y + \pi)(y - 3\pi)(z + \pi)(z - 3\pi)$$

The computation domain is $[-\pi, 3\pi]^3$, and zero Dirichlet B.C. has been used. The history of the converging error is shown in the left of Fig. 3, the dash line corresponding to no preconditioning, and the solid line corresponding to with preconditioning. Using preconditioning the speed is about three times faster as

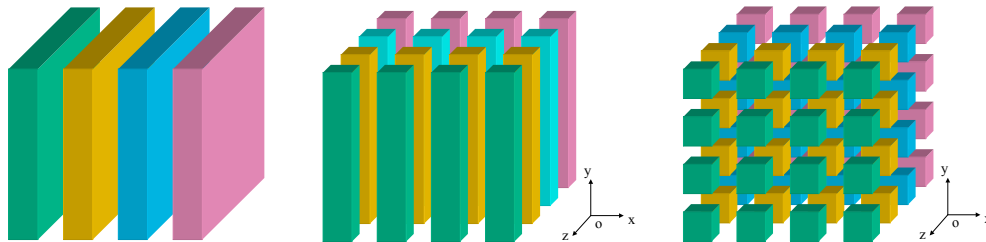


Fig. 2: Three parallel models (A, B and C) for solving Poisson's equation using Fourier method

as a powerful tool to analyses multi-scale phenomena. We have developed a Poisson solver using wavelet expansions. A MRA of consists of a chain of closed subspaces

before. Using wavelet, there are only few percent of total coefficients are larger than some critical value, as shown on the middle of Fig. 3.

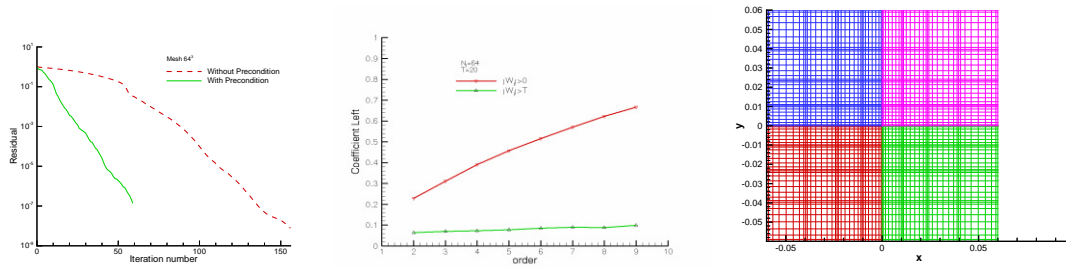


Fig. 3: Convergence history with/out preconditioning (left), wavelet coefficients (middle) and 2D structured grid (right)

Domain decomposition has also been used for parallelization, and relatively good scaling has been achieved. It has also been incorporated into PTRACK code, nearly the same results have been obtained.

Spectral Element Method on Structured Grid

The Spectral Element Method (SEM) originated in the 1980's [6, 7, 8], and has been applied in many different areas. In our Vlasov solvers, a parallel Poisson solver based on Spectral Element Method (SEM) on structured grid has been constructed. 2D structured grid has been shown on the right of Fig. 3. 2D bases have been shown on the left of the Fig. 4. Similarly, domain decomposition has been used for parallelization with Dirichlet boundary conditions. Continuous Galerkin (CG) method has been used and zero Dirichlet B.C. has been imposed. Due to the memory limitation, only the iterative solver can be used for solving boundary modes of the 2D Poisson's equation when the mesh is large. Interior modes in each element have been solved directly according to the Shur complement. The discrete system of Poisson's equation can be written as: (b and i correspond to boundary and interior variables)

$$\begin{pmatrix} A_{bb} & C_{bi} \\ C_{bi}^T & A_{ii} \end{pmatrix} \begin{pmatrix} u_b \\ u_i \end{pmatrix} = \begin{pmatrix} f_b \\ f_i \end{pmatrix}$$

$$(A_{bb} - C_{bi} A_{ii}^{-1} C_{bi}^T) u_b = f_b - C_{bi} A_{ii}^{-1} f_i$$

$$u_i = A_{ii}^{-1} (f_i - C_{bi}^T u_b)$$

Figure 4 (middle) and (right) show the charge and

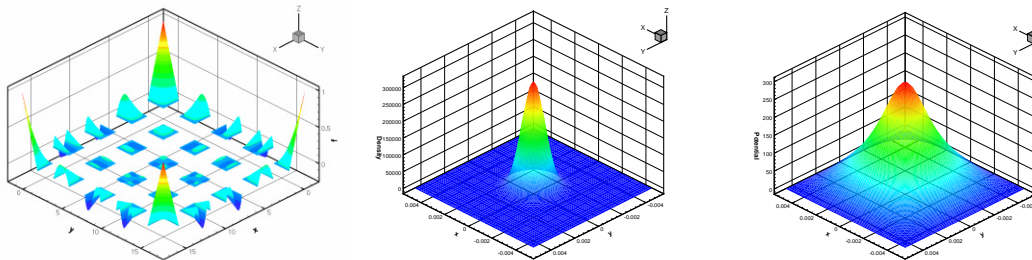


Fig. 4: Modal bases (left) on 2D structured grid, charge (middle) and potential (right) distributions

potential distributions. Since zero Dirichlet B.C. has been used, the potential is nonzero close to the boundary. This means the domain size need large enough to obtain the right potential distribution.

Spectral Element Method on Unstructured Grid

In order to solve Poisson in complex geometries, a parallel Poisson solver using SEM on an unstructured grid has been developed recently. Since finite element method (FEM) can handle complex geometry easily, and spectral method can achieve high order accuracy. Combine these two, SEM can handle the complex geometry and also achieve high order accuracy at the same time.

The potential can be expressed as

$$f(r, s) = \sum_{i+j \leq p} \psi_{ij}(r, s) \hat{f}_{ij}$$

The continuous Galerkin formula for solving the Poisson's equation is

$$\begin{aligned} \int_V f \cdot \phi dv &= \int_V \nabla^2 u \cdot \phi dv \\ &= \int_V [\nabla \cdot (\nabla u \phi) - \nabla u \cdot \nabla \phi] dv \\ &= \int_{\partial V} \bar{n} \cdot (\nabla u \phi) dS - \int_V \nabla u \cdot \nabla \phi dv \\ \int_V \nabla u \cdot \nabla \phi dv &= \int_{\partial V} \bar{n} \cdot (\nabla u \phi) dS - \int_V f \cdot \phi dv \\ \int_{\partial V} \bar{n} \cdot (\nabla u \phi) dS &= \int_{\partial V} (n_x \phi \frac{\partial u}{\partial x} + n_y \phi \frac{\partial u}{\partial y}) dS \end{aligned}$$

A mesh partition for 4 processors has been shown on the left of Fig. 5. Middle and right plots in Fig. 5 show the charge and potential distributions on a circular domain.

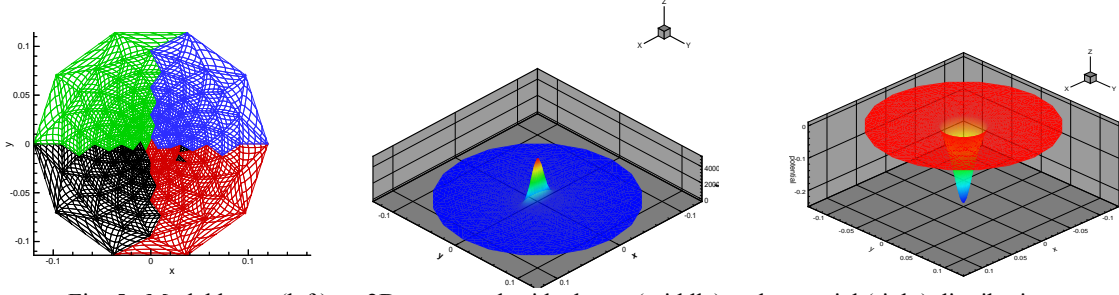


Fig. 5: Modal bases (left) on 2D structured grid, charge (middle) and potential (right) distributions

DYNAMIC SIMULATION WITH VLASOV SOLVERS

In order to overcome the shortcoming of the PIC solvers, we have developed direct Vlasov solvers. The distribution function $f(\vec{x}, \vec{v}, t)$ in phase space is governed by the Vlasov equation.

Vlasov equation in 1P1V phase space

In 1P1V phase space, the non-dimensional Vlasov equation can be written as following:

$$\frac{\partial f(x, v, t)}{\partial t} + v(x, t) \frac{\partial f(x, v, t)}{\partial x} + E(x, t) \frac{\partial f(x, v, t)}{\partial v} = 0$$

$$E(x, t) = -\frac{\partial \phi(x, t)}{\partial x}, -\Delta \phi(x, t) = \frac{\partial E(x, t)}{\partial x} = \rho(x, t) - 1$$

$$\rho(x, t) = \int_{-\infty}^{\infty} f(x, v, t) dv$$

Vlasov equation in 2P2V phase space

In beam dynamics, a simplified model can be deduced in 2P2V form as a paraxial model based on the following assumptions:

- The beam is in a steady-state: All partial derivatives with respect to time vanish;
- The beam is sufficiently long so that the longitudinal self-consistent forces can be neglected;
- The beam is propagating at a constant velocity v_b

along the propagation axis z ;

- Electromagnetic self-forces are included;
- $\vec{p} = (p_x, p_y, p_z)$, $p_z \sim p_b$ and $p_x, p_y \ll p_b$

where $p_b = \gamma m v_b$ is the beam momentum. It follows in particular that

$$\beta \approx \beta_b = (v_b / c)^2, \gamma \approx \gamma_b = (1 - \beta_b^2)^{-1/2}$$

- The beam is narrow: the transverse dimensions of the beam are small compared to the characteristic

longitudinal dimension. The paraxial model can be written as:

$$\frac{\partial f}{\partial z} + \frac{\vec{v}}{v_b} \cdot \nabla_{\vec{x}} f + \frac{q}{\gamma_b m v_b} \left(-\frac{1}{\gamma_b^2} \nabla \Phi^s + \vec{E}^e + (\vec{v}, v_b)^T \times \vec{B}^e \right) \cdot \nabla_{\vec{v}} f = 0$$

Coupled with Poisson's equation

$$-\Delta_{\vec{x}} \Phi^s = \frac{q}{\epsilon_0} \int_{R^2} f(z, \vec{x}, \vec{v}) d\vec{v}$$

where Φ^s is the self-consistent electric potential due to charges. \vec{E}^e and \vec{B}^e are external electric and magnetic fields. v_b is the reference beam velocity.

Numerical Algorithm

The Semi-Lagrangian Method (SLM) [9] has been used for time integration. A plot explains the idea has been shown on the left of Fig. 7. The time splitting scheme has been used for time integration as proposed by Cheng and Knorr [10].

- ```

.....
Do istep=1, nstep:
- Compute $\rho(x, t) = \int f(x, v, t) dv$;
- Compute $E^{pred} = E^n - j^n \Delta t$ from Ampere's law;
- Do until $|E^{N=1} - E^{pred}| < \epsilon$
 · Substep1: $v^{n+1/2} = v^{n+1} - E^{pred}(x^{n+1}) \Delta t / 2$
 · Substep2: $x^n = x^{n+1} - v^{n+1/2} \Delta t$;
 · Substep3: $v^n = v^{n+1/2} - E^n(x^n) \Delta t / 2$;
 · Interpolate to compute charge density;
 · Solve Poisson's equation for E^{n+1} ;
 · Update new $E^{pred} = E^{n+1}$.
- Enddo
Enddo
.....

```

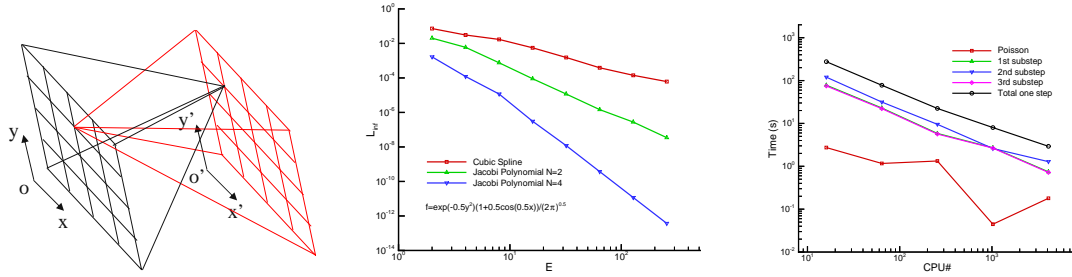


Fig. 6: 4D domain decomposition (left), Interpolation errors vs. element number (middle) and strong scaling in 2P2V simulation (right)

The algorithm for 2P2V simulation is similar to the above, but with advancing the first and the last substeps in physical space and the second substep in the velocity space.

Table 1. Scaling 2D Poisson solver ( $E=64$ ,  $P=4$ )

| CPU      | 16  | 64  | 256  | 1024 | 4096  |
|----------|-----|-----|------|------|-------|
| Time (s) | 286 | 68  | 17.2 | 4.08 | 1.66  |
| PE       | 1.0 | 1.0 | 1.0  | 1.0  | 0.673 |

### Benchmarks and Simulation Results

The code comprises two major parts: interpolation and space charge (SC) calculation. The SLM performs back tracking and interpolation respectively in the physical and velocity spaces. Each processor has only part of the global mesh for the space charge calculations. The field mesh and space charge mesh are different. This scheme has the advantage of easy implementation and no communication for particle tracking is required. However, this method requires large memory in each processor and intense communication for the parallel Poisson solver. Figure 6 (left) shows the domain decomposition in 4D for 2P2V simulations.

Table 1 shows the benchmark results for the 2D Poisson solver. Good scaling has been achieved. Figure 6 (middle) compares the interpolation errors with cubic spline, Jacobi polynomial with  $P=2$  and 4. Clearly using a Jacobi polynomial gives much better results, which is good to use in the Semi-Lagrangian scheme. The right plot in Fig. 6 shows the strong scaling results for both the Poisson and Vlasov solvers in 2P2V simulations. It

shows that the Vlasov solver can have good scaling because the most time consuming part is the interpolation. And since the interpolations are local on each processor, there is no communication between different processors. So even when the scaling of the Poisson solver becomes worse with 4k processors, the overall scaling is still good.

The middle and right figures in the Fig. 7 show the time history of  $\log(E_x)$  for linear and strong Landau damping. The initial particle distribution function and the related parameters are shown in following:

$$f(0, x, v) = \frac{1}{\sqrt{2\pi}} \exp(-v^2/2)(1 + \alpha \cos(kx))$$

$$\forall(x, v) \in [0, L] \times R, \quad \alpha = 0.01, \quad k = 0.5$$

$$L = 4\pi, \quad R = [-6, 6], \quad \Delta t = 1/8,$$

$$P = 16, \quad E = 64, \quad 1024 \times 1024$$

$$CPU = 256, \quad T \sim 10 \text{ min } s$$

For the linear Landau damping,  $\alpha=0.01$ , and for the strong Landau damping,  $\alpha$  is 0.5. Clearly they represent different dynamics. The decreasing and increasing rate can be measured and are consistent with theoretical predictions and other researchers.

### 2P2V Simulations

In 2P2V simulations, a proton beam has been simulated through alternating hard edge electric quadrupole channel. The initial emittance is  $\varepsilon = 200\pi$  mm mrad, and the energy is  $W=0.2$  MeV. The current of the beam is 0.1 A, and the reference velocity is  $v_b = 6.19 \times 10^6$  m/s. The transverse physical space is  $[-0.12, 0.12]$  by  $[-0.12, 0.12]$ , and the velocity space is

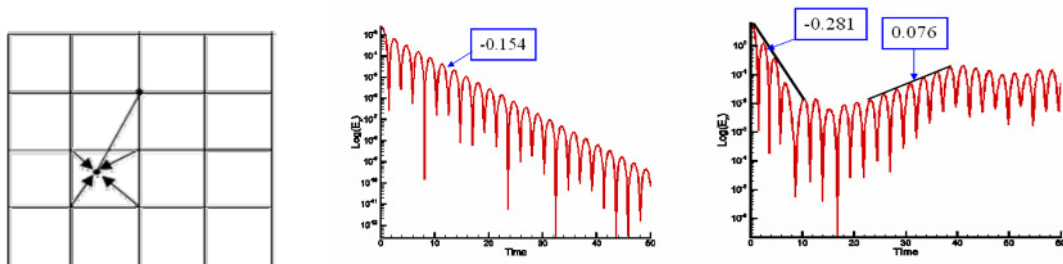


Fig. 7: Semi-Lagrange Scheme (left), Linear Landau Damping (middle), Strong Landau Damping (right)



$[-8 \times 10^5, 8 \times 10^5]$  by  $[-8 \times 10^5, 8 \times 10^5]$  m/s. The alternating electric quadrupole field is defined as  $\vec{E}^e(x, y, z) = (k_0(z)x, -k_0(z)y)$  and shown in Fig. 8.

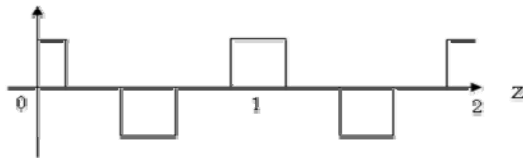


Fig. 8: Alternating electric focusing force

Since the initial beam distribution is Gaussian (not a KV distribution), the RMS envelope is not periodic with the amplitude fluctuating from one period to the next. Figure 9 shows the beam contours in  $(x, y)$ ,  $(x, x')$ ,  $(y, y')$  and  $(x', y')$  phase planes at  $z=0$  and 192 steps. Detailed information on 1P1V and 2P2V Vlasov simulations can be found in [2].

### SUMMARY

This paper presents our researches on beam dynamic simulations with PIC method, different parallel Poisson solvers, and beam dynamic simulations with direct Vlasov solvers. Domain decomposition has been adopted for parallelization of TRACK code, and several parallel Poisson solvers have been developed and incorporated into PTRACK. PTRACK has now been used for large scale beam dynamic optimization and simulations. Several numerical techniques have been used to solve Poisson's equation in different conditions, such as using Cartesian and Cylindrical coordinate systems, using structure and unstructured grids, etc. Direct Vlasov solvers have been developed with a high-order SEM. The advantages and effectiveness of the SEM have been demonstrated. The Vlasov solvers have adopted the Semi-Lagrangian method. Similarly domain decomposition has been used for parallelization of these solvers. Scalable Poisson solvers have been developed within. Benchmarks of the parallel models have shown good scaling on BlueGene/P at ANL with up to 4k processors. The SEM shows its advantages in these direct Vlasov solvers, such as local interpolation, easy parallelization and long time integration. These explorations are encouraging, and more investigation will be done.

### REFERENCES

[1] P.N. Ostroumov, V. N. Aseev, and B. Mustapha. Phys. Rev. ST. Accel. Beams 7, 090101 (2004).  
 [2] J. Xu and P.N. Ostroumov, Computer Physics Communications, 178 (2008) 290-300.  
 [3] J. Xu, B. Mustapha, V.N. Aseev and P.N. Ostroumov, Phys. Rev. ST. Accel. Beams 10, 014201 (2007).  
 [4] J. Xu, B. Mustapha, V. N. Aseev and P.N. Ostroumov, HB 2008, Nashville, Tennessee, USA, Aug. 25- 29, 2008.  
 [4] M. Gutnic, M. Haefele, I. Paun and E. Sonnendrücker, Comput. Phys. Comm., 164, 214-219 (2004).

[5] E. Sonnendrücker, J. Roche, P. Bertrand and A. Ghizzo, J. Comput. Phys., 149, 201 (1998).  
 [6] F. Filbet, E. Sonnendrücker, Vol.16, No.5, 763-791 (2006).  
 [6] M.O. Deville, P.F. Fischer and E.H. Mund, High-Order Methods for Incompressible Fluid Flow, Cambridge University Press, Cambridge (2002).  
 [7] J.S. Hesthaven and T.Warburton, Nodal Discontinuous Galerkin Methods: Algorithms, Analysis and Applications, Springer, New York (2008).  
 [8] G.E. Karniadakis and S.J. Sherwin, Spectral/hp element methods for CFD, Oxford University Press, London (1999).  
 [9] A. Robert, Atmos. Ocean. 19, 35 (1981).  
 [10] C.Z. Cheng and G. Knorr, J. Sci. Comp., 22, 330 (1976).

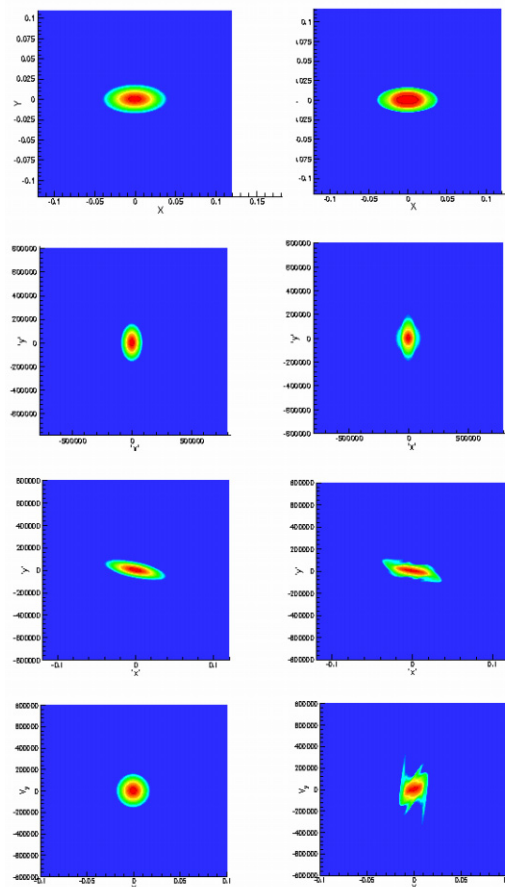


Fig. 9: From top to bottom are contours in the  $(x, y)$ ,  $(x, x')$ ,  $(y, y')$  and  $(x', y')$  planes, from left to right correspond to  $z=0$  and 192 time steps.